

A Chemical Pump that Generates High-Pressure Gas by Transmitting Liquid Fuel against Pressure Gradient

Junsoo Kim, Kai Luo, and Zhigang Suo*

A pneumatic soft robot can be made autonomous by carrying a liquid chemical fuel. In the existing design, to transmit the fuel, the pressure of the fuel tank must exceed that of the actuator. Consequently, the fuel tank must be sufficiently stiff, which hardens the robot. Herein, inspired by pit membranes in trees, a chemical pump is developed, which is consisting of a nanoporous membrane between the fuel tank and the actuator, and coated with a catalyst on the side of the actuator. The fuel in the fuel tank migrates across the membrane and, on meeting the catalyst, decomposes into a pressurized gas and inflates the actuator. The chemical pump is driven by the free energy of reaction, against the difference in pressure. The pores in the membrane are large enough for the fuel molecules to migrate through, but small enough to block the pressurized gas to tunnel back. In a demonstration, the fuel tank has ambient pressure, and the actuator has a pressure of 350 kPa, comparable to the pressure in a car tire. The chemical pump enables pneumatic robots to be autonomous, powerful, and soft.

1. Introduction

Pneumatic soft robots achieve complex and powerful motion.^[1,2] Making these robots autonomous, however, has been challenging. Pneumatic pumps, such as electric air compressors, are commonly used with tethered tubes.^[1–7] In a few cases, the robots are made autonomous by carrying the pneumatic pump and battery, but these components make robots hard and heavy.^[8,9] Alternatively, liquid fuels have been used as a power source of soft robots.^[10–14] The fuels, such as hydrocarbons and hydrogen peroxide, generate pressurized gas, which inflates actuators. The liquid chemical fuels have a relatively high energy

density compared to other power sources, which would enable autonomous soft robots to be compact and powerful (batteries $\approx 2 \text{ MJ kg}^{-1}$, $\text{H}_2\text{O}_2 \approx 3 \text{ MJ kg}^{-1}$, gasoline $\approx 40 \text{ MJ kg}^{-1}$).^[15,16]

In one existing design, the fuel tank and the actuator are connected through a tube (Figure 1a). To inflate the actuator, the fuel tank must be pressurized more than the actuator, so that the fuel tank should be stiffer than the actuator. Incidentally, a check valve prevents backflow but cannot transmit the fuel if the fuel tank has a lower pressure than the actuator.^[17] The fuel tank is elastically deformed to pressurize the liquid fuel. As the fuel is consumed, the fuel tank deflates, which lowers the power of the actuator. In another existing design, the actuator is vented before the fuel is injected into the actuator, closed with a

valve, and detonated.^[11–14] Such a design does not require a highly pressurized fuel tank but is limited to pop-like actuation. These requirements and limitations cannot be resolved by using a small and hard fuel tank. For example, even though the fuel tank is hard, the pressure of the fuel tank still should be higher than the pressure of the actuator to transmit the fuel. The power will be attenuated as the pressure of the fuel tank decreases. Furthermore, small fuel tanks cannot carry lots of fuel. Here, we develop a chemical pump to transmit a liquid fuel from a low-pressure tank to high-pressure actuator (Figure 1b). We characterize the chemical pump and demonstrate its use by using two latex balloons. Our work solves a fundamental limitation in designing autonomous pneumatic soft robots that carry liquid fuel.


2. Result

2.1. Pit Membranes in Trees

In developing the chemical pump, we have been inspired by the ascent of water in a tree.^[18] When the water in the tree is in equilibrium, the pressure of water at the top of the tree relates to that at the bottom of the tree by $P_{\text{top}} = P_{\text{bottom}} - \rho gh$, where ρ is the density of water, g is gravitational acceleration, and h is the height of the tree. Assume that water at the bottom is under atmospheric pressure, $P_{\text{bottom}} = 100 \text{ kPa}$. For a tree of height $h = 100 \text{ m}$, gravity causes a pressure difference of $\rho gh \approx 1 \text{ MPa}$. Consequently, water at the top of the tree is under negative pressure (i.e., tension) of $\approx 1 \text{ MPa}$ and is vulnerable to

J. Kim, Z. Suo
J. A. Paulson School of Engineering and Applied Sciences
Harvard University
Cambridge, MA 02138, USA
E-mail: suo@seas.harvard.edu

K. Luo
MOE Key Laboratory of Dynamics and Control of Flight Vehicle
School of Aerospace Engineering
Beijing Institute of Technology
Beijing 100081, China

 The ORCID identification number(s) for the author(s) of this article can be found under <https://doi.org/10.1002/aisy.202100246>.

© 2022 The Authors. Advanced Intelligent Systems published by Wiley-VCH GmbH. This is an open access article under the terms of the Creative Commons Attribution License, which permits use, distribution and reproduction in any medium, provided the original work is properly cited.

DOI: 10.1002/aisy.202100246

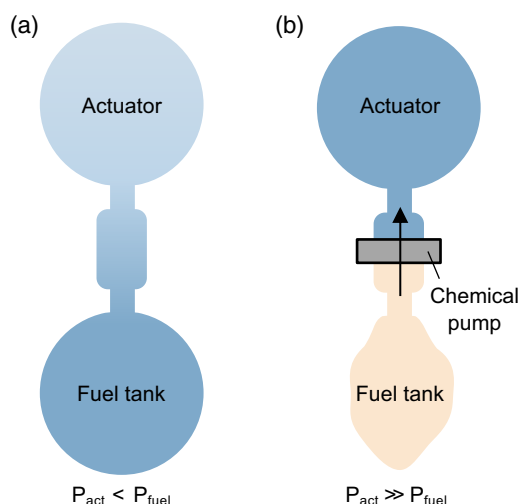


Figure 1. Transmit a liquid fuel from a fuel tank to an actuator. a) When the fuel tank and the actuator are simply connected, the pressure of the fuel tank must exceed that of the actuator. b) When the fuel tank and the actuator are connected with a chemical pump, the pressure of the fuel tank can be lower than that of the actuator.

cavitation. Once a cavity forms, the tension in the water will cause the cavity to grow. If water were transported through a single tube from the bottom to the top of the tree, one cavity would break the water column and dry the entire tree. The tree solves this problem by a system of short tubes (Figure 2a–d).^[19] Each tube is connected to multiple other tubes by nanoporous pit membranes. When all the tubes are filled with water, water can transport across the pit membranes. When a cavity forms in a tube, water vapor will fill the tube at the saturation pressure of ≈ 2.3 kPa. The large difference in the pressure of the vapor in the tube and the tension of water in the surrounding tubes is sustained by the nanopores in the pit membrane. The maximum pressure that the nanopores can hold is given by the Laplace pressure, $2\gamma/a$, where γ is the surface tension of water, and a is the radius of the pores. For representative values, $\gamma \approx 0.1 \text{ N m}^{-1}$ and $a \approx 10 \text{ nm}$, the Laplace pressure is 10 MPa, sufficient to sustain the tension in water. The pores in the pit membrane are large enough for the fuel molecules to migrate through, but small enough to prevent the gas bubbles from tunneling back.

2.2. Design of a Chemical Pump

The pit membrane inspires the design of our chemical pump. A chemical pump consists of a nanoporous membrane, which separates the fuel tank and actuator (Figure 2e). The fuel tank is filled with liquid hydrogen peroxide. Spread on the surface of the membrane facing the actuator are platinum particles, which catalyze the fuel to decompose. A hydrogen peroxide molecule is much smaller than the size of a nanopore and can migrate through the membrane. Upon meeting the platinum particles, hydrogen peroxide liquid decomposes into water vapor and oxygen gas. The mixture of gasses is highly pressurized but is confined by the nanoporous membrane. In the membrane, hydrogen peroxide is concentrated less at the side facing the

actuator than at the side facing the fuel tank. This difference in chemical potential pumps hydrogen peroxide to migrate across the membrane. The highly pressurized gases inflate the actuator, but the fuel tank needs not to be pressurized.

A polyacrylamide gel is used as a nanoporous membrane. Hydrogen peroxide and water can form a solution of any proportion and can be used as a solvent in the polyacrylamide gel. For a gas bubble to invade the membrane, the pressure of the gas must exceed the Laplace pressure, $2\gamma/a$ (Figure 2f).^[20] In the case of the polyacrylamide gel, $a \approx 10 \text{ nm}$ is the mesh size, and $\gamma \approx 0.1 \text{ N m}^{-1}$ is the surface tension of the hydrogen peroxide solution, so that the Laplace pressure is on the order of 10 MPa, which is sufficiently high for soft robots. Some gas molecules may dissolve in the membrane and penetrate by diffusion, but the amount of diffusion of gas is negligible. For example, at the pressure of the actuator of 400 kPa, the concentration of oxygen molecules in the gel is four orders of magnitude lower than the concentration of the fuel.

In a tree, for water to permeate through a pit membrane with low resistance, the membrane is thin, on the order of 100 nm. For such a thin membrane to sustain a high pressure difference, the membrane has a small diameter, on the order of microns, and is supported by the wall of the tubes. We mimic this design by placing the polyacrylamide gel on a nylon mesh. The gel functions as a pit membrane, and the nylon mesh functions as the wall (Figure S1, Supporting Information). We choose a nylon mesh because it is flexible but strong enough to resist the high pressure of the gas (Figure 2g). The maximum pressure that the chemical pump can operate depends on the thickness of the gel h , space between nylon fibers s , and diameter of the nylon fibers d , as well as the shear modulus of the membrane μ .

2.3. Simulation of the Deformation of the Membrane

To aid the design, we simulate the deformation and stress using a commercial finite-element package, ABAQUS (Figure 3a, Note S1, Supporting Information). The deformation decreases as s/d decreases or h/d increases. Also, when $h/s > 1$, the normalized stress $\sigma/\mu < 3$, and the central region is almost stress-free. When $h/s < 1$, the stress drastically increases. The weakest geometry ($s/d = 2$ and $h/d = 0.5$) is not displayed, because it cannot sustain the pressure. We further plot the normalized displacement of the bottom middle point u/d as a function of $\Delta P/\mu$ (Figure 3b). The slope indicates how much the nanoporous membrane deforms due to the pressure. The slope decreases as h/d increases or s/d decreases. When $s/d = 2$ and $h/d = 0.5$, u/d diverges at $\Delta P/\mu = 1.5$. When $s/d = 1$, u/d is insensitive to h/s when $h/s > 2$. Therefore, the nanoporous membranes do not need to be thicker than $2s$.

2.4. Characterization of a Chemical Pump

We characterize a chemical pump using a homemade experimental setup (Figure 4a,b, Figure S2, Supporting Information). A gel membrane and a nylon mesh separate a fuel tank and a chamber of a fixed volume. When the fuel migrates across the gel membrane and decomposes into gases into the chamber, the gas pressure is recorded by a pressure sensor.

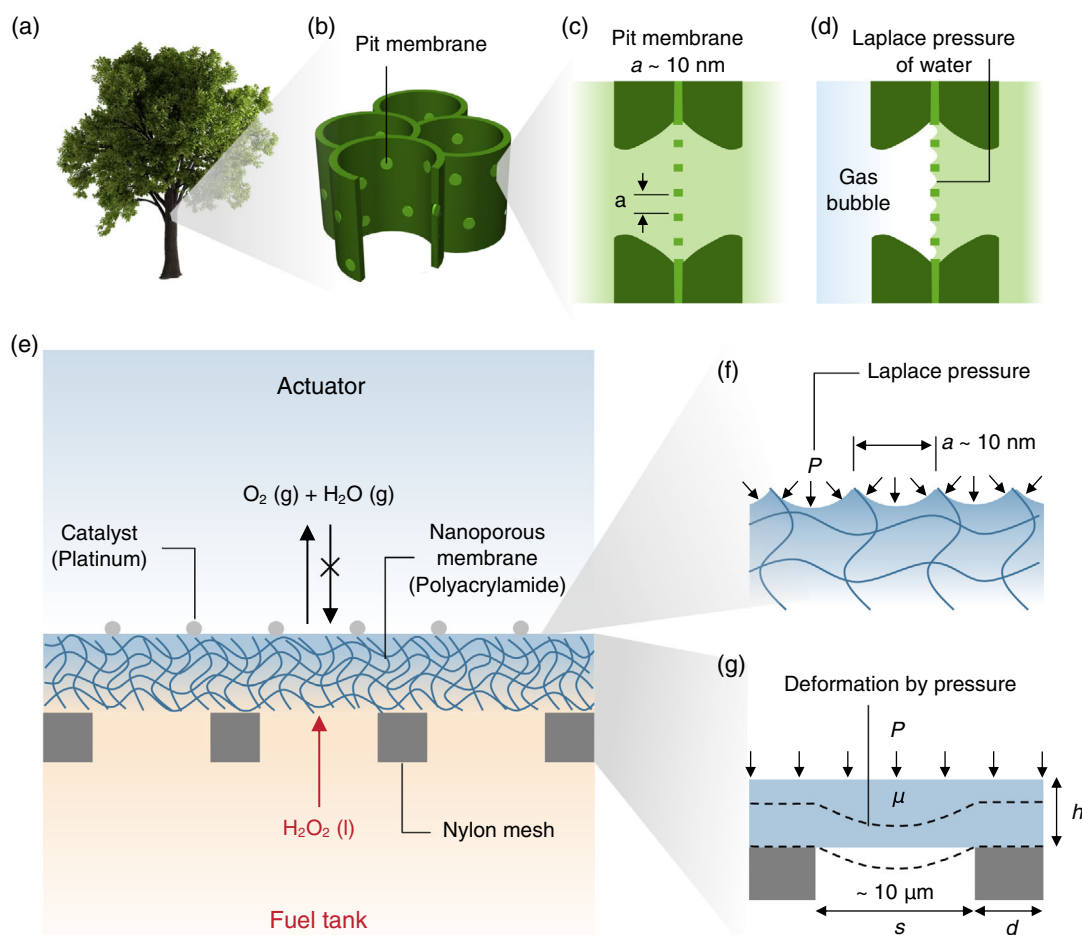


Figure 2. The pit membrane of a tree inspires the design of a chemical pump. a) Water transports from the bottom to top of a tree through many short tubes. b) Each tube is connected to multiple other tubes through nanoporous pit membranes. c) When the tubes on both sides of a pit membrane are filled with water, the pores in the membrane are large enough to transport water. d) When one tube is filled with gas, but the other tube is filled with water, the pores in the membrane are small enough to block gas bubbles. e) Schematic of a chemical pump. A nanoporous membrane is placed on a nylon mesh, and separates an actuator and a fuel tank. The fuel tank contains hydrogen peroxide. Upon diffusing through the membrane and meeting the catalyst (platinum particles), the fuel decomposes into oxygen gas and water vapor. f) The nanoporous membrane blocks gas bubbles. g) The nylon mesh supports the nanoporous membrane.

After the reaction, $\text{H}_2\text{O}_2 \rightarrow \text{H}_2\text{O} + 1/2\text{O}_2$, the membrane is hot, and the water molecules are in the gas phase (Figure S3, Supporting Information). The chamber has a large surface area and is kept approximately at room temperature through the experiment, so that most of the water molecules condense into a liquid. We assume that the change of the pressure in the chamber is entirely due to the oxygen gas produced by the reaction. In the reaction, the number of reacted hydrogen peroxide molecules is twice the number of oxygen molecules. We calculate the reaction rate dm/dt from the ideal gas law, $dm/dt = 2M(kT)^{-1} V(dP/dt)$, where m is the mass of the reacted hydrogen peroxide, M is the mass per hydrogen peroxide molecule, kT is the temperature in the unit energy, and V is the volume of the chamber. The reaction rate divided by the area of the gel defines the reaction flux.

We characterize the chemical pump as a function of several parameters, including pressure difference ΔP , thickness of the

membrane h , concentration of hydrogen peroxide in the fuel, and crosslinker density of the membrane (i.e., a weight ratio of crosslinker to the monomer), and density of catalyst (i.e., mass of platinum particles per unit area). Unless otherwise noted, we use the following values of parameters: $h = 150 \mu\text{m}$, H_2O_2 concentration = 30 wt%, crosslinker density = 1.45 wt%, and catalyst density = 24 g m^{-2} . When the crosslinker density is 1.45 wt%, the shear modulus of the membrane is $\mu = 50 \text{ kPa}$, which is expected to be able to support ΔP of $\approx 300 \text{ kPa}$ according to the finite-element analysis ($s/d = 0.55$ and $h/d = 4.5$). This value is sufficiently high for most soft robots. The modulus of soft materials is on the order of 100 kPa – 1 MPa . Usually, the thickness of the soft actuator is 1%–10% of the diameter of the actuator. Therefore, even the gas of 300 kPa would apply a hoop-stress of 3–30 MPa at the soft material, which is near the strength of most soft materials.

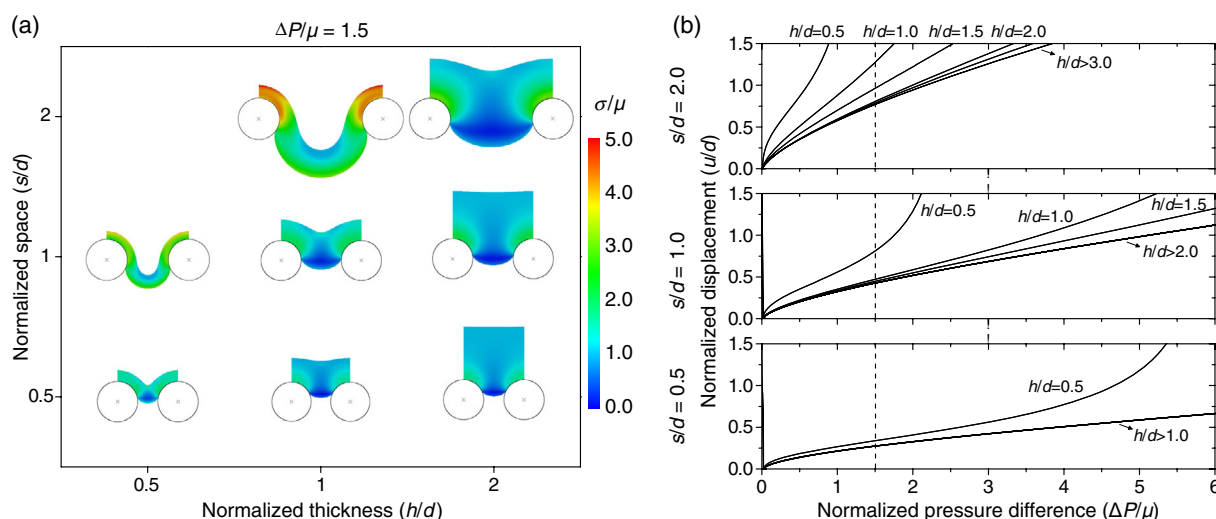


Figure 3. Finite element simulation of chemical pumps. a) Chemical pumps of various geometric parameters s/d and h/d at a normalized pressure $\Delta P/\mu = 1.5$. b) Normalized displacement of the bottom middle point of the membrane u/d as a function of the normalized pressure $\Delta P/\mu$.

We prepare the chemical pump with a membrane of polyacrylamide hydrogel, without hydrogen peroxide. We then use a pipette to dispense the fuel on the membrane and measure the pressure over time. As the fuel migrates through the membrane, the rate of pressure, dP/dt , increases and becomes nearly linear in a few seconds (Figure 4c). This behavior is in good agreement with the solution of the partial differential equation of diffusion (Note S2, Supporting Information). The pressure keeps increasing until the membrane fails. One of the failure modes is fracture of membrane due to excessive deformation, as discussed in the simulation. As we predict the maximum pressure of 400 kPa earlier, we terminate the experiment by venting the chamber at ≈ 350 kPa, so that the membrane does not rupture. The reaction flux is then calculated from the rate of pressure.

We show the reaction flux as a function of the pressure of the chamber (Figure 4d, $h = 240$ μm). In this experiment, the data are obtained after several tests. Since the membrane contains some fuel migrated at the previous experiment, the reaction flux rapidly increases at the beginning of the experiment. As the pressure builds up, the reaction flux reaches the maximum value, decreases about 10%, and becomes constant. The chemical pump keeps producing gas at a high pressure of 350 kPa, which is comparable to the pressure in a car tire. The apparent overshoot of the reaction flux at low pressure may be because the nylon mesh stretches and increases the volume of the chamber as the pressure increases. The high partial pressure of oxygen negligibly affects the reaction flux, because the Gibbs free-energy difference of the reaction is high.^[21] The reaction flux can be predicted by the model used in Figure 4c.

Because the fuel is transported by diffusion, the reaction flux is expected to be inversely proportional to h . Thus, we can enhance the reaction flux by using a thinner nanoporous membrane (Figure 4e). The diffusion of the fuel also depends on h/d . We include this effect as a boundary condition in solving the differential equation (Figure S4, Supporting Information). The

measured reaction flux as a function of h is in good agreement with the prediction.

The reaction flux increases as the concentration of H_2O_2 in the fuel tank increases (Figure 4f). When the concentration of H_2O_2 in the fuel tank is low, the reaction flux is linear in the concentration, as expected from the simple model on the basis of Fick's law. When the concentration is high, the reaction flux becomes nonlinear, and the simple model of diffusion is no longer valid. When the concentration is too high (80 wt% of H_2O_2), the heat of the reaction damages the membrane and the nylon mesh. With polyacrylamide and nylon mesh, we have achieved a reaction flux of ≈ 10 $\text{g m}^{-2}\text{s}^{-1}$. The reaction flux can be further increased by using more concentrated fuel, thinner membrane, and more thermally stable materials.

We measure the reaction flux as a function of the crosslinker density of the membrane (Figure 4g). When the crosslinker density is low, the cavities form in the membrane, and the reaction flux is reduced (Figure S5, Supporting Information). This observation is consistent with the observation that the mass flux of the hydrogen peroxide through the vapor in the cavities is lower than through the liquid in the gel. When the crosslink density is higher than 0.4 wt%, the cavities no longer form. The reaction flux under this condition fits with the prediction of the model. We also measure the reaction flux as a function of the density of the catalyst (Figure 4h). As the density of the catalyst increases, the reaction flux increases, and then plateaus around the density of the catalyst of 15 g m^{-2} . This plateau is reached when the platinum particles are too many to attach to the surface (Figure S6, Supporting Information). The reaction flux at the plateau fits with the prediction of the model.

The materials for the chemical pump are not limited to the polyacrylamide gel and the nylon mesh. For example, we have also used a hydrophilic filter paper and a stainless steel mesh (Figure S7, Supporting Information). The device used for Figure S7, Supporting Information, has lower reaction flux than that shown in Figure 4 and lower Laplace pressure, but achieves

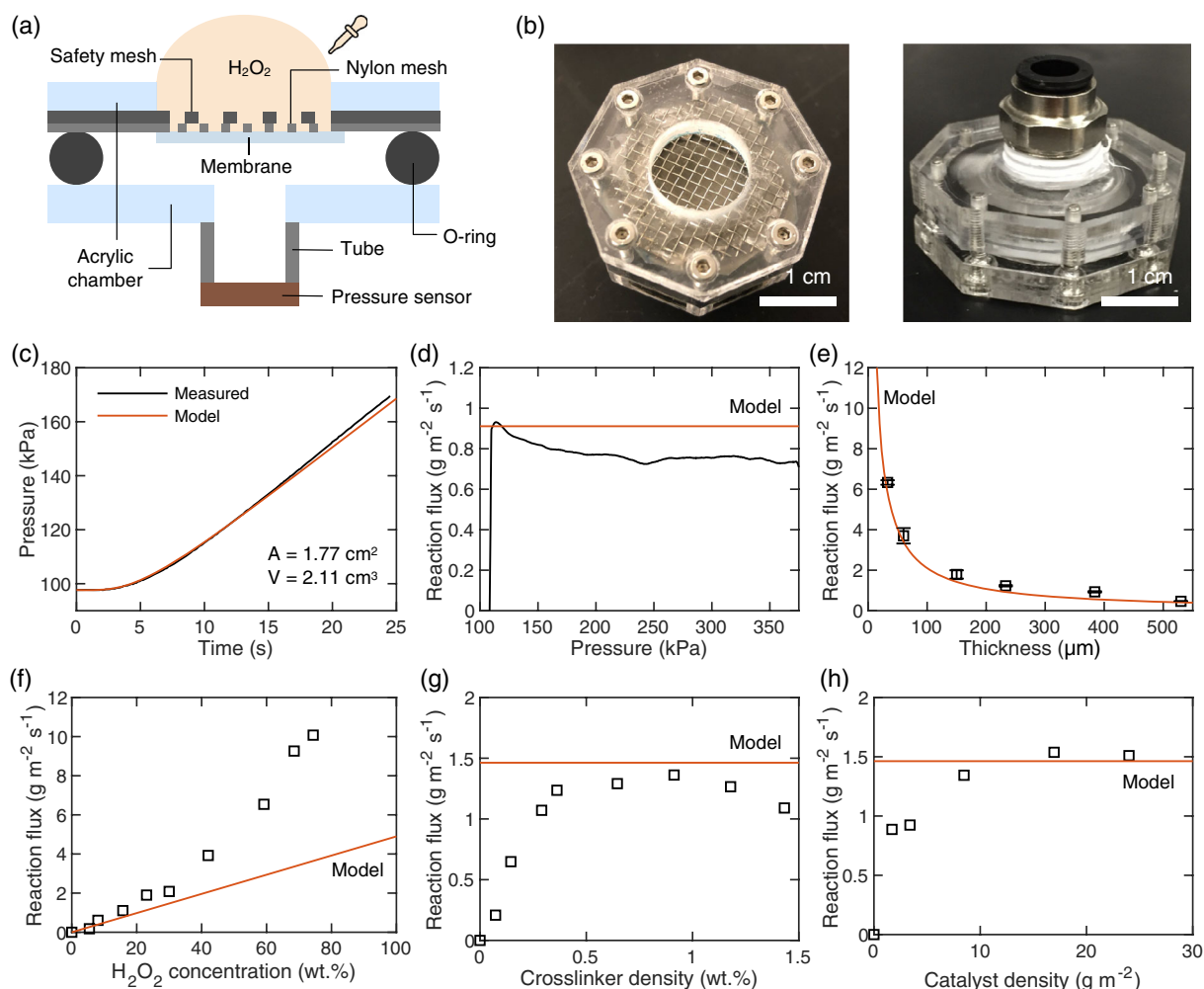


Figure 4. Characterization of a chemical pump. a) The schematic of an experimental setup. A gel membrane, supported by a nylon mesh, separates a fuel tank and a chamber of a fixed volume. For safety, we put a metal mesh over the nylon mesh. When the fuel migrates across the gel membrane and decomposes on the top surface, the gas pressure in the chamber is recorded by a pressure sensor, and the reaction flux is calculated according to the ideal gas law. b) Photographs of the top and bottom of the equipment. For visual clarity, the tube and the pressure sensor are not included. c) The pressure is measured as a function of time. The reaction flux depends on d) the pressure of the actuator, e) the thickness of the membrane, f) the concentration of the fuel, g) the crosslinker density of the membrane, and h) the density of the catalyst. The predictions of a model are compared with the experimental data (c–h).

the key features of chemical pumps: pumping fuels, generating gas of high pressure, and decoupling of pressures. Various materials enable choices of pores size, stiffness, porosity, and range of thermal stability for broad applications.

Instead of the power density, we can also estimate the area required to inflate unit volume per second, without a load. For example, consider the reaction flux of $10 \text{ g m}^{-2} \text{ s}^{-1}$ (Figure 4f). As two hydrogen peroxide molecules generate one oxygen molecule, the flux of generation of gas molecules is $0.147 \text{ mol m}^{-2} \text{ s}^{-1}$. To inflate the actuator with the pressure difference of 100 kPa, the number of gas molecules in the actuator per volume at room temperature is $P/RT = 40.3 \text{ mol m}^{-3}$. Therefore, with the unit area, it takes 274 s to inflate unit volume. To inflate the 10 mL (10^{-5} m^3) pneumatic actuator with 1 Hz (1 s), we need an area of 27.4 cm^2 ($5.2 \text{ cm} \times 5.2 \text{ cm}$). As we can fold the membrane many times to increase the area, the size

of the chemical pump can be made small. In steady state, the reaction flux is the same as the flux through the membrane, that is, the mass of liquid crossing the membrane per unit time per unit area. For a representative flux in our experiment, $10 \text{ g m}^{-2} \text{ s}^{-1}$, with the density of the fuel, $\approx 1 \text{ g mL}^{-1}$, the flux can also be given as $10 \text{ mL m}^{-2} \text{ s}^{-1}$. When the concentration of the fuel is 30 wt% and the area is $7.85 \times 10^{-5} \text{ m}^2$, the flow rate of the hydrogen peroxide in our setup is 236 nL s^{-1} .

We have not quantitatively tested the service life of the chemical pump. However, when the actuator pressure is lower than the critical value that breaks the membrane and the fuel flow rate is below the critical value that damages the membrane, we have not seen failure during our experiments. For example, we have recorded the pressure for a day and repeated the actuation more than twenty times, the chemical pump worked normally.

2.5. Demonstration of a Chemical Pump

Consider two latex balloons, one serving as a fuel tank, and the other serving as an actuator (**Figure 5**, Figure S8a,b, Movie S1 and S2, Supporting Information). The fuel tank is softer than the actuator. Without the chemical pump, the fuel tank and the actuator have equal pressure, so that the decomposition of the hydrogen peroxide inflates the fuel tank but not the actuator (Figure 5a). Any disturbance of the fuel tank, such as a squeeze, disturbs the actuator (Figure 5b). The pressure in the actuator cannot exceed the pressure in the fuel tank. Once the fuel tank is damaged, both the fuel in the fuel tank and the gas in the actuator leak (Figure 5c).

With the chemical pump, by contrast, the pressures in the fuel tank and the actuator decouple, so that the fuel tank does not inflate even when it is softer than the actuator (Figure 5d).

A squeeze on the fuel tank does not disturb the actuator (Figure 5e). Once the fuel tank is damaged, the gas in the actuator does not leak (Figure 5f). Also, we demonstrate a strong actuation by using fuel of ambient pressure (Figure 5g,h, Movie S3, Supporting Information). The pneumatic actuator (Figure S8c, Supporting Information) is connected to the chemical pump. When a pipette dispenses the fuel on the chemical pump, the fuel migrates across the chemical pump, decomposes into gases, pressurizes the actuator, and lifts 1.5 kg of weights. The pressure in the actuator exceeds the ambient pressure by 80 kPa.

Under the reversible conditions, the free energy of reaction is converted to mechanical work. However, existing demonstrations (including ours) considerably deviate from the reversible conditions. Irreversibility results from dissipation associated with change in temperature, diffusion of the fuel through the

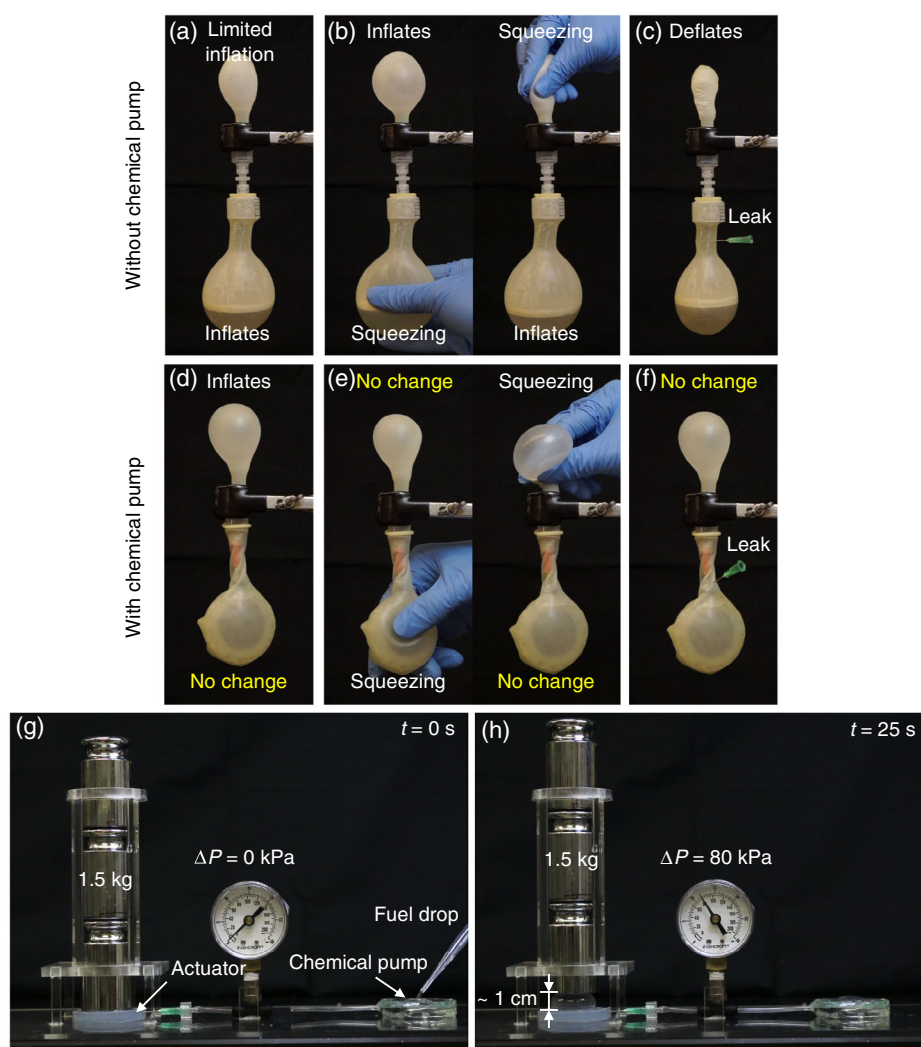


Figure 5. Demonstrations of the chemical pump. Two latex balloons are simply connected. One serves as an actuator, and the other serves as a fuel tank. a) The actuator does not operate if the fuel tank is softer than the actuator. b) Any disturbance on one part disturbs the other. c) Both the fuel and the gas leak if the fuel tank is damaged. Two latex balloons are connected with the chemical pump. d) The actuator operates regardless of its stiffness. e) There is no interference. f) The fuel tank does not leak the gas in the actuator. g) The fuel of ambient pressure is dispensed on the chemical pump. h) The soft actuator lifts 1.5 kg of weights under 80 kPa of pressure difference.

membrane, friction between moving parts, and viscoelasticity of the soft actuator. In addition, part of the work is stored as elastic energy in the soft actuator, and only a fraction of the energy is used in actuation (i.e., lifting a weight). The efficiency of an actuator can be defined by the ratio of the energy of actuation to the free energy of reaction. Because the diffusion of H_2O_2 through the membrane dissipates a small amount of energy, the efficiency of the chemical pump is comparable to that of the actuator by direct decomposition of H_2O_2 . At room temperature, the free energy of the reaction, $\text{H}_2\text{O}_2 \rightarrow \text{H}_2\text{O} + 1/2\text{O}_2$, is 3 MJ kg^{-1} .^[15] The energy of actuation can be measured by the potential energy of lifting a mass to a certain height. A representative value in our experiment is the energy of actuation of 150 mJ upon consuming $\approx 1 \text{ mL}$ of 30 wt% fuel. Consequently, the efficiency of our actuator is $\approx 10^{-4}$. This efficiency may be compared to an efficiency of $\approx 10^{-3}$ reported for a jumping soft robot by combustion of methane.^[15]

3. Conclusion

A chemical pump can transmit a liquid fuel from a low-pressure tank to a high-pressure actuator. The size of the pores in the membrane is large enough for the liquid fuel to migrate through, but is small enough to prevent the pressurized gas from tunneling back. Chemical pumps will also be useful when multiple pneumatic actuators are used. Without a chemical pump, all actuators are directly connected to the fuel tank, share the pressurized gas, and are coupled. Although regulators are used, the pressure of the actuator cannot exceed the pressure of the fuel tank, and an actuator can disturb the other actuators. By contrast, with chemical pumps, all actuators can operate independently at different pressures, which allows a complex motion.

In our system, the fuel reacts continuously because the membrane is coated with the catalyst. The reaction stops when the catalyst is detached from the membrane, and resumes when the catalyst is in contact with the membrane. Therefore, the pump can be controlled on demand for a complex motion by changing the location of the catalyst. For example, the catalyst can be relocated if it is in the form of a mesh instead of being spread particles. When the catalyst mesh touches the membrane, the fuel will decompose. When the catalyst mesh is detached from the membrane, the reaction will stop. The position of the mesh can be changed by a small force, so the control can be realized by various low-energy actuators.^[8] The integration of such a control mechanism with the actuator is beyond the scope of this paper.

Hydrogen peroxide has been used in many soft robot systems, as it can be easily decomposed into gases by using catalysts at room temperature, and the fire has not been an issue yet.^[22] One possible reason is that the water molecules produced together with the oxygen molecules may reduce the risk of fire significantly. Other monopropellant fuels, such as hydrazine, can also generate gas by themselves but is carcinogenic, which limits the use of these fuels in soft robots.^[23] Various hydrocarbons, such as methane and butane, have also been an energy source of pneumatic soft robots.^[15] These fuels also emit relatively high energy when they combust but require oxygen molecules for

combustion. The oxygen can be replenished from the environment like previous soft robots using hydrocarbon fuels. Also, the oxygen can be provided into the actuator by reacting hydrogen peroxide together. A different fuel needs a different design for a chemical pump. For this reason, we fix a type of fuel in this paper and focus on how the chemical pump can provide fuel against the pressure gradient and its benefits.

We have used polyacrylamide and nylon mesh to demonstrate the chemical pump, but other materials can also be used. The chemical pump can consist of diverse materials of different porosity, rigidity, geometry, and thermal stability, and can be optimized for specific applications. Soft autonomous robots can be softer and safer but more powerful by using chemical pumps.

4. Experimental Section

Preparation of the Membrane: The polyacrylamide hydrogel was used as a nanoporous membrane. Acrylamide of 42.65 g (monomer) was dissolved in 300 mL of deionized water (Poland Spring), 0.925 g of N,N' -Methylenebisacrylamide (crosslinker) was dissolved in 60 mL of deionized water, and 0.1461 g of α -ketoglutaric acid (photoinitiator) was dissolved in 10 mL of deionized water to make 2, 0.1, and 0.1 M stock solution, respectively. We prepared a precursor by mixing these solutions. The ratio between the monomer solution and the photoinitiator solution was fixed to 1:0.02 in volume. The crosslinker solution was added according to the values of the density of the crosslinkers. To make a gel membrane, commercial plastic films with different thicknesses were used as spacers. After pouring the precursor onto the glass plate with the spacer, we exposed UV light (365 nm, 10 ea of 8 W bulbs, Sankyo) for 2 h. We submerged the gel membrane in the deionized water to swell to equilibrium. Platinum particles of 30 mg (Sigma-Aldrich, 327476) were mixed with 1 mL of hexane (Sigma-Aldrich) and then dispensed using a pipette. To disperse the agglomerated particles, we dropped 30 wt% hydrogen peroxides (Sigma-Aldrich) onto the particles. The generated gas dispersed the agglomerate particles and spread them. The gel membrane was then placed on a nylon mesh (McMaster-Carr, 307 mesh). The nylon mesh had a dimension of $d = 33 \mu\text{m}$ and $s = 50 \mu\text{m}$.

Preparation of the Chemical Pump: We prepared the membrane and the nylon mesh with a diameter of 5 cm. We cut acrylic sheets to make rings and used them to hold the nylon mesh. For safety, we prepared the polyethylene terephthalate (PET) mesh and supported the nylon mesh. The design of each component was described in Figure S8a, Supporting Information. Materials were cut by using a Laser cutter (Epilog Helix). To seal the nylon mesh, the edge of the nylon mesh was filled with UV curable resin, NOA73 (Figure S8b, Supporting Information). The gel was placed on the nylon mesh, and the edge of the membrane was glued to NOA 73 with Krazy glue. We spread the platinum particles on the membrane, and dispersed by dispensing a small amount of hydrogen peroxide on the agglomerated particles. We assembled the acrylic rings and the bottom substrate by using epoxy glue, and connected to the actuator through a silicon tube.

Preparation of the Soft Actuator: We placed the PET film on the Sylgard 186 substrate, and poured more precursor of Sylgard 186 on the PET film. After curing, we separated the Sylgard 186 substrate and the PET film by using a needle, and connected it to the tube.

Measurement of the Reaction Flux: Acrylic sheets (McMaster-Carr) were cut by using a laser cutter (Epilog Helix) and assembled by using O-ring and screws. The pressure was measured by using a Pressure Sensor 400 (Vernier) with Go!Link (Vernier). We used 30 wt% hydrogen peroxide (Sigma-Aldrich) as fuel and concentrated it by distillation when necessary. Details on the materials and methods were available in the Supporting Information.

Supporting Information

Supporting Information is available from the Wiley Online Library or from the author.

Acknowledgements

The authors thank S. Zhou and R. Bai for the discussion. This work at Harvard was supported by the NSF MRSEC (DMR-2011754). J.K. acknowledges financial support from a Kwanjeong Educational Foundation. K.L. is supported by China Scholarship Council as a visiting scholar for one year at Harvard University.

Conflict of Interest

The authors declare no conflict of interest.

Data Availability Statement

The data that support the findings of this study are available in the supplementary material of this article.

Keywords

autonomous robots, chemical pumps, fuels, pneumatic actuators, soft robots

Received: November 29, 2021

Revised: January 7, 2022

Published online:

- [1] G. M. Whitesides, *Angew. Chem.* **2018**, 49, 280.
- [2] D. Yang, B. Mosadegh, A. Ainla, B. Lee, F. Khashai, Z. Suo, K. Bertoldi, G. M. Whitesides, *Adv. Mater.* **2015**, 27, 6323.
- [3] S. I. Rich, R. J. Wood, C. Majidi, *Nat. Electron.* **2018**, 1, 1.
- [4] B. Mosadegh, P. Polygerinos, C. Keplinger, S. Wennstedt, R. F. Shepherd, U. Gupta, J. Shim, K. Bertoldi, C. J. Walsh, G. M. Whitesides, *Adv. Funct. Mater.* **2014**, 24, 2163.
- [5] R. L. Truby, M. Wehner, A. K. Grosskopf, D. M. Vogt, S. G. M. Uzel, R. J. Wood, J. A. Lewis, *Adv. Mater.* **2018**, 521, 1706383.
- [6] G.-Z. Yang, J. Bellingham, P. E. Dupont, P. Fischer, L. Floridi, R. Full, N. Jacobstein, V. Kumar, M. McNutt, R. Merrifield, B. J. Nelson, B. Scasellati, M. Taddeo, R. Taylor, M. Veloso, Z. L. Wang, R. Wood, *Sci. Robot.* **2018**, 3, eaar7650.
- [7] F. Ni, D. Rojas, K. Tang, L. Cai, T. Asfour, *IEEE Int. Conf. Robot. Autom.* IEEE, Piscataway, NJ **2015**, pp. 3154–3159.
- [8] D. Rus, M. T. Tolley, *Nature* **2015**, 521, 467.
- [9] V. Cacucciolo, J. Shintake, Y. Kuwajima, S. Maeda, D. Floreano, H. Shea, *Nature* **2019**, 572, 516.
- [10] M. Wehner, R. L. Truby, D. J. Fitzgerald, B. Mosadegh, G. M. Whitesides, J. A. Lewis, R. J. Wood, *Nature* **2016**, 536, 451.
- [11] M. Loepfe, C. M. Schumacher, U. B. Lustenberger, W. J. Stark, *Soft Robot.* **2015**, 2, 33.
- [12] M. T. Tolley, R. F. Shepherd, M. Karpelson, N. W. Bartlett, K. C. Galloway, M. Wehner, R. Nunes, G. M. Whitesides, R. J. Wood, in *IEEE/RSJ Int. Conf. on Intelligent Robots and Systems (IROS)*, IEEE, Chicago, IL **2014**, pp. 561–566.
- [13] R. F. Shepherd, A. A. Stokes, J. Freake, J. Barber, P. W. Snyder, A. D. Mazzeo, L. Cademartiri, S. A. Morin, G. M. Whitesides, *Angew. Chem.* **2013**, 52, 2892.
- [14] N. W. Bartlett, M. T. Tolley, J. T. B. Overvelde, J. C. Weaver, B. Mosadegh, K. Bertoldi, G. M. Whitesides, R. J. Wood, *Science* **2015**, 349, 161.
- [15] M. Wehner, M. T. Tolley, Y. Mengüç, Y.-L. Park, A. Mozeika, Y. Ding, C. Onal, R. F. Shepherd, G. M. Whitesides, R. J. Wood, *Soft Robot.* **2014**, 1, 263.
- [16] J. M. Tarascon, M. Armand, *Nature* **2001**, 414, 359.
- [17] B. Mosadegh, C.-H. Kuo, Y.-C. Tung, Y. Torisawa, T. Bersano-Begey, H. Tavana, S. Takayama, *Nat. Phys.* **2010**, 6, 433.
- [18] T. D. Wheeler, A. D. Stroock, *Nature* **2008**, 455, 208.
- [19] J. S. Sperry, V. Stiller, U. G. Hacke, *Agron. J.* **2003**, 95, 1362.
- [20] S. Kundu, A. J. Crosby, *Soft Matter* **2009**, 5, 3963.
- [21] R. Serra-Maia, M. Bellier, S. Chastka, K. Tranhuu, A. Subowo, J. D. Rimstidt, P. M. Usov, A. J. Morris, F. M. Michel, *ACS Appl. Mater. Interfaces* **2018**, 10, 21224.
- [22] M. Shi, E. M. Yeatman, *Microsystems Nanoeng.* **2021**, 7, 95.
- [23] T. G. McGee, J. W. Raade, H. Kazerooni, *J. Dyn. Syst. Meas. Control* **2004**, 126, 75.